Boundary singularities produced by the motion of soap films

Raymond E. Goldstein, James McTavish, H. Keith Moffatt[1], and Adriana I. Pesci

Department of Applied Mathematics and Theoretical Physics, University of Cambridge, Cambridge CB3 0WA, United Kingdom

Contributed by H. Keith Moffatt, April 9, 2014 (sent for review February 10, 2014)

Recent work has shown that a Möbius strip soap film rendered unstable by deforming its frame changes topology to that of a disk through a "neck-pinching" boundary singularity. This behavior is unlike that of the catenoid, which transitions to two disks through a bulk singularity. It is not yet understood whether the type of singularity is generally a consequence of the surface topology, nor how this dependence could arise from an equation of motion for the surface. To address these questions we investigate experimentally, computationally, and theoretically the route to singularities of soap films with different topologies, including a family of punctured Klein bottles. We show that the location of singularities (bulk or boundary) may depend on the path of the boundary deformation. In the unstable regime the driving force for soap-film motion is the mean curvature. Thus, the narrowest part of the neck, associated with the shortest nontrivial closed geodesic of the surface, has the highest curvature and is the fastest moving. Just before onset of the instability there exists on the stable surface the shortest closed geodesic, which is the initial condition for evolution of the neck's geodesics, all of which have the same topological relationship to the frame. We make the plausible conjectures that if the initial geodesic is linked to the boundary, then the singularity will occur at the boundary, whereas if the two are unlinked initially, then the singularity will occur in the bulk. Numerical study of mean curvature flows and experiments support these conjectures.

minimal surfaces | topological transitions | systoles

The study of singularities, be it their dynamic evolution (1–3) or their location and structure in a system at equilibrium (4, 5), has a long history. The main focus of research has been either on systems without boundaries, where both the static and dynamic cases are fairly well understood, or on finite systems with prescribed boundaries displaying static singularities, as for example defects in liquid crystals (6) and superfluids (7), Langmuir monolayers (8), and quantum field theories (9). Work on dynamic aspects of these bounded systems is limited, particularly in the case of singularity formation accompanying a topological change (10). For instance, to our knowledge, there is no mathematical tool available to predict from initial conditions whether a singularity in a bounded system will occur in the bulk or at the boundary.

In a previous paper (11) we found that a soap film in the shape of a Möbius band spanning a slowly deforming wire would change its topology through a singularity that occurs at the boundary. This simple example provided a first model to investigate the dynamical aspects of the formation of a boundary singularity from the moment the system becomes unstable, and until a new stable configuration is reached. While progress was made in the particular case of the Möbius band, left unanswered were questions of greater generality: (*i*) Are there any other configurations of films spanning a frame that have a topology transition with a boundary singularity, showing that this behavior is generic rather than exceptional? (*ii*) If so, what are the possible types of evolution equations that could describe the dynamics of the collapse? (*iii*) When such a system becomes unstable, can topological and geometric parameters at onset be used to predict whether the singularity will occur in the bulk or at the boundary? As described below, we have found that the first question has an affirmative answer. Just as Courant (12, 13) used soap films as a means of studying minimal surface topology, we can seek to answer these questions through the study of soap-film transition singularities.

The evolution of bulk singularities and of soap films moving toward equilibrium configurations have been extensively studied (14) with mean curvature flow in which the surface moves normal to itself at a speed proportional to the local mean curvature and also with models more faithful to hydrodynamics (15, 16). There is also a large body of literature pertaining to the case of closed surfaces for which rigorous results have been proved (17–20). In contrast, the dynamics of a surface with a deformable boundary which, after becoming unstable, undergoes a singular topological change has received little or no attention, particularly when the singularity occurs at the boundary.

To study the dynamical aspects of boundary singularities and their relationship to the topological and geometric parameters of the film, we performed numerical calculations based on mean curvature flow and verified that, even though the actual motion of a film also involves inertial and more realistic viscous forces, this approach is capable of reproducing the essential characteristics of the boundary singularities we observed in experiment. This stands in clear contrast with the case of bulk singularities, where the mean curvature approach fails to fully reproduce the experimental observations. For example, a film collapsing in the bulk by mean curvature produces one singularity, whereas in experiment there are at least two placed above and below a satellite drop (21–23).

The best-known example of such a bulk singularity in a bounded soap film is the collapse of a catenoid spanning two parallel rings. In this case the singularity occurs only when the rings have been separated beyond a critical distance and the film, as it becomes unstable, develops a narrow neck on which a noncontractible curve of least length, or systole relative to the boundary (SRB)

Significance

The dynamics of topological rearrangements of surfaces are generically associated with singularities. It is not yet understood whether the location of a singularity (in the bulk or at boundaries) is a general consequence of the surface topology, nor how this dependence could arise from an equation of motion for the surface. Here we use experiments on soap films, computation, and theory to introduce simple and intuitive concepts to describe generic transitions and their singularities. In particular, we propose a criterion to predict, from the configuration of the initial state, the location of the singularity. This criterion involves the topological linkage between the bounding curve of the surface and a local systole, the local nontrivial minimum-length closed curve on the surface.

Author contributions: R.E.G., J.M., H.K.M., and A.I.P. designed research, performed research, and wrote the paper.

The authors declare no conflict of interest.

Freely available online through the PNAS open access option.

[1]To whom correspondence should be addressed. E-mail: hkm2@damtp.cam.ac.uk.

This article contains supporting information online at www.pnas.org/lookup/suppl/doi:10.1073/pnas.1406385111/-/DCSupplemental.

(24–26), can be found. Even though the collapse of the catenoid is a situation characterized by high symmetry, we will see here, through a combination of experiment and computation, that there is a whole class of singularities that follow the same pattern of neck formation such that infinitesimally close to but before the onset of the instability it is possible to identify a local SRB (LSRB) that constitutes the initial condition for the evolution of the curve whose contraction ends at the location of the singularity (see Fig. 5). We find that this feature of the initial LSRB and its linkage to the boundary makes it possible to deduce whether the singularity occurs in the bulk or at the boundary, and also that the way in which the same boundary is deformed before onset of the instability can produce different types of singularities.

Results and Discussion

1. Experiments. In previous work (11) it was found that when a soap film in the shape of a Möbius band becomes unstable, it collides with its frame via a neck-like singularity. This collision yields changes in three topological quantities: the genus, the sidedness, and the linking number between the Plateau border and the frame (for details, see ref. 11). These experiments could not, by themselves, establish if there was causality in these results, so we sought other film configurations to test which of the topological parameters, if any, are predictors of the transition. One such configuration starts from the surface first introduced by Almgren (27) [(a) in Fig. 1]. This film has the interesting feature of having an intersection along a segment that can develop into a secondary film by slightly pushing the descending tab. The direction in which the tab is pushed determines if the secondary film lies toward the front or the back [(a.1) and (a.ii) in Fig. 1, respectively]. As illustrated, the two possible resolutions of the unstable fourfold vertex into the films in (a.1) and (a.ii) in Fig. 1 correspond to the two stable states which, in the language of foams, interconvert through a T1 process (28). Puncturing the secondary film when it lies toward the front produces the well-known result (27) shown in (b) in Fig. 1, which is topologically equivalent to a section of a torus. On the other hand, puncturing the secondary film when it lies toward the back produces a surface [(c) in Fig. 1] that we believe has not been identified before in this context, and which corresponds to a punctured Klein bottle, i.e., two Möbius bands of opposite chirality sewn together over part of their boundaries. It is this latter surface that we used to test our hypotheses. This punctured Klein bottle (hereafter termed "punctured Klein") is an ideal choice because, like the Möbius band (linking number 2, nonorientable genus 1), it is one sided, but its Plateau border linking number with the frame is 0 and its nonorientable genus is 2, allowing us to separate the two topological parameters.

By pulling apart the top sections of the frame in (c) in Fig. 1 the punctured Klein becomes unstable and undergoes a transition to a disk by means of two mirror image singularities. This transition, which is identical to two simultaneous Möbius transitions of opposite chirality, becomes fully dynamical after onset and once it has finished [(c.ii), or equivalently (c.i.2), in Fig. 1], the parameters that have changed are the sidedness and the genus. There are at least two other alternative routes from the punctured Klein to the disk. The second route, although much harder to realize experimentally, is very intuitive mathematically: Since the punctured Klein is made of two sewn Möbius bands, it is possible to first coerce the frame into collapsing one of the bands producing a change of nonorientable genus from 2 to 1 and also from linking number 0 to ± 2, and leaving as a result only one of the Möbius bands of the original pair [(c.i.1) in Fig. 1]. Hence the surface is still one sided. The last part of the process is the usual Möbius collapse that will yield the two-sided disk [(c.i.2) in Fig. 1] and will again change both the genus and the linking number to 0, as expected. In the end the features of the collapse to a final two-sided disk can be distilled to those of the two individual Möbius bands that made the whole, and as a consequence each one of these two steps is a fully dynamical process. The fact that any other film that can be constructed in such a way that it consists of a series of Möbius bands sewn together can be analyzed in a similar manner hints to the possibility of constructing a simple algebra to keep track of the net changes of the topological parameters of the surface at every stage of the collapse. The third way to convert the punctured Klein into a disk requires deforming the boundary quasistatically by pulling the tab upward slowly until its tip rises above the plane of the horizontal film [(c.iii.1–c.iii.3) in Fig. 1]. Along this route, unlike along the other two, the process can be stopped at any instant of time and there

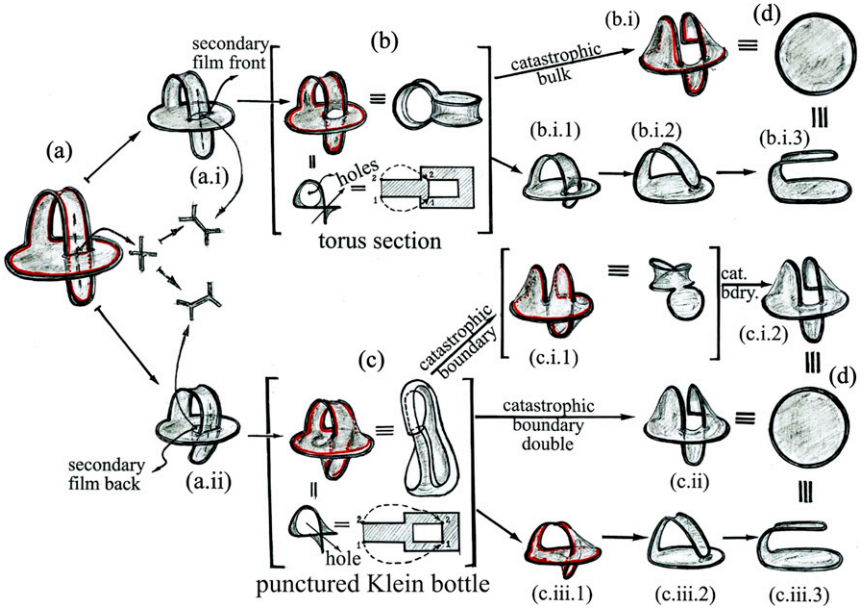

Fig. 1. Interconversions of various soap film topologies, as described in *Results and Discussion*. Shaded regions are films, and red lines denote locations of Plateau borders. This figure shows how surface (a) can reach the final configuration (d), a disc topology, following five distinct routes.

will always be a stable minimal surface that spans the frame. When the tip of the tab finally reaches the horizontal plane, the twists of the Plateau borders and the holes of the film will all converge to a point (the location of the singularity). The twists will annihilate each other because they are of opposite chirality and the hole will vanish to a point. In the physical film the hole would disappear by reconnecting. All these different routes to the end result share the feature that the singularity always occurs at the boundary.

In the same way in which a whole class of transitions in the bulk reduces asymptotically to the neck-like transition of the catenoid, we expect that a whole class of boundary transitions of one-sided surfaces will reduce to the neck-like transition of a Möbius band. Thus, studying the collapses of these two surfaces should be sufficient to cover all possible types of neck-like singularities.

There are three possible types of collapse:

i) Quasistatic boundary singularity: The surface changes its topology in such a way that a stable, minimal surface can be found at every instant before and up to the time of the singularity which occurs at the boundary.
ii) Catastrophic bulk singularity: The surface changes its topology after becoming unstable. Hence, the process is fully dynamic and there are no intermediate stable minimal surfaces visited in-between the last stable surface before onset and until the final stable surface is reached. In this case the singularity is located in the bulk.
iii) Catastrophic boundary singularity: The same as *ii* except that the singularity occurs at the boundary.

While there is a fourth possibility—a quasistatic bulk singularity—we have not found a film configuration where this is observed. The different types of singularities have a specific correlation with the change of topology, but beyond the change of genus, there is no one-to-one correspondence between the type of transition and the topological parameters. The rules that govern the transitions are

a) In a catastrophic boundary singularity there is a change in either the linking number or sidedness, or both.
b) If a change of linking number or sidedness occurs there is a boundary singularity, either catastrophic or quasistatic.
c) A catastrophic bulk singularity can change neither the linking number nor the sidedness of the surface.
d) A quasistatic boundary singularity can support any type of topological change.

From our studies it appears that both types of catastrophic singularities, bulk and boundary, can be transformed into a boundary quasistatic singularity by choosing a suitable frame deformation. For example, for the catenoid, instead of pulling the rings apart to render the film unstable and force the transition to two disks, we can tilt the top ring quasistatically until it reaches a position where the film touches itself and the boundary, thus creating a pair of disks connected by a single point. The connection point is the location of the singularity that occurs as the two disks are finally separated.

The experiments also helped with the study of another feature of these films that is connected with geometric characteristics of the associated minimal surfaces. In general, when films that will collapse through a neck-like singularity are made, they come out of the soap solution with a secondary film spanning the neck (Fig. 2 *A*, *C*, and *E*). This feature was highlighted by Almgren (27), who named the shared curve between the main and secondary films the "singular set." If the secondary film is allowed to remain while the wire is deformed, it is possible to contract it to a point so that the final surface is identical to the one that would have been obtained if the secondary film were removed at the start of the process. Because soap films minimize area, it is clear that the location of the singular set is also the location of the shortest closed noncontractible geodesic on the main film. In fact, we observe that secondary films generically occur in situations where the main film supports the existence of such a curve. When the secondary film contracts during a transition, this geodesic shrinks and eventually reduces to a point which coincides with the location of the singularity. Not surprisingly, in the absence of the secondary film, the shortest closed geodesic of the main film is close to the original singular set. In a physical film the shortest closed geodesic in the main film is, however, longer than the curve determined by the singular set due to the effect of surface tension.

2. Theoretical and Numerical Results. In this section we first address whether motion by mean curvature is capable of reproducing the experimental observations of boundary singularities in the collapse of Möbius band and punctured Klein surfaces. This requires mathematical representations of boundary curves for the two cases which contain parameters describing the deformations leading to surfaces instabilities. For the Möbius band, we have previously identified (11) the one-parameter family of curves $C_M : \mathbf{x}(\theta) = (x, y, z)$ with $\mu = -1$ and $0 \le \theta < 2\pi$, where (29)

$$x(\theta) = \frac{1}{\ell_M}\left[\mu\tau\cos\theta + (1-\tau)\cos 2\theta\right], \qquad \textbf{[1a]}$$

$$y(\theta) = \frac{1}{\ell_M}\left[\mu\tau\sin\theta + (1-\tau)\sin 2\theta\right], \qquad \textbf{[1b]}$$

$$z(\theta) = \frac{1}{\ell_M}\left[2\mu\tau(1-\tau)\sin\theta\right]. \qquad \textbf{[1c]}$$

Here, the parameter τ $(0 \le \tau \le 1)$ interpolates smoothly from the double covering of the circle for $\tau = 0$ to a single circle in the x–y plane when $\tau = 1$. The factor $\ell_M(\tau)$ normalizes the wire length to 2π. Numerical studies with Surface Evolver (30) show that the one-sided minimal surface spanning this curve becomes unstable when $\tau > \tau_{1c} \simeq 0.398$, whereas the two-sided surface becomes unstable for $\tau < \tau_{2c} \simeq 0.225$. In-between these values the system is bistable, with the energies of the two surfaces crossing at $\tau \simeq 0.38$.

The frame shown in (a) in Fig. 1, which can support the punctured Klein surface [(c) in Fig. 1], can be approximated by a two-parameter family of curves $C_K : \mathbf{x}(\theta) = (x, y, z)$ for $0 \le \theta < 2\pi$, where

$$x(\theta) = \frac{1}{\ell_K}\left\{\cos\theta + \frac{1}{2}\cos\left[t\ \mathrm{e}^{-\lambda\sin^2\theta/2}\right]\right\}, \qquad \textbf{[2a]}$$

$$y(\theta) = \frac{1}{\ell_K}\sin\theta, \qquad \textbf{[2b]}$$

$$z(\theta) = \frac{1}{2\left(1+\sin^2\theta/2\right)\ell_K}\sin\left[t\ \mathrm{e}^{-\lambda\sin^2\theta/2}\right], \qquad \textbf{[2c]}$$

and $\ell_K(t, \lambda)$ is again a normalization, here depending on the two parameters of the curve. As shown in Fig. 3, the parameter t primarily controls the length of the tab below the plane of the circle, while λ controls the width of the tab.

Collapse dynamics. In each of these cases a dynamical evolution toward the singularity was obtained by starting with an equilibrium shape close to the critical parameter(s) for instability and then incrementing one of the parameter(s) a small amount beyond the threshold. The subsequent evolution of the surface was calculated using the Hessian command in Surface Evolver (30) with repeated equiangulations and vertex averaging to ensure a well-behaved mesh. In both the Möbius and punctured Klein

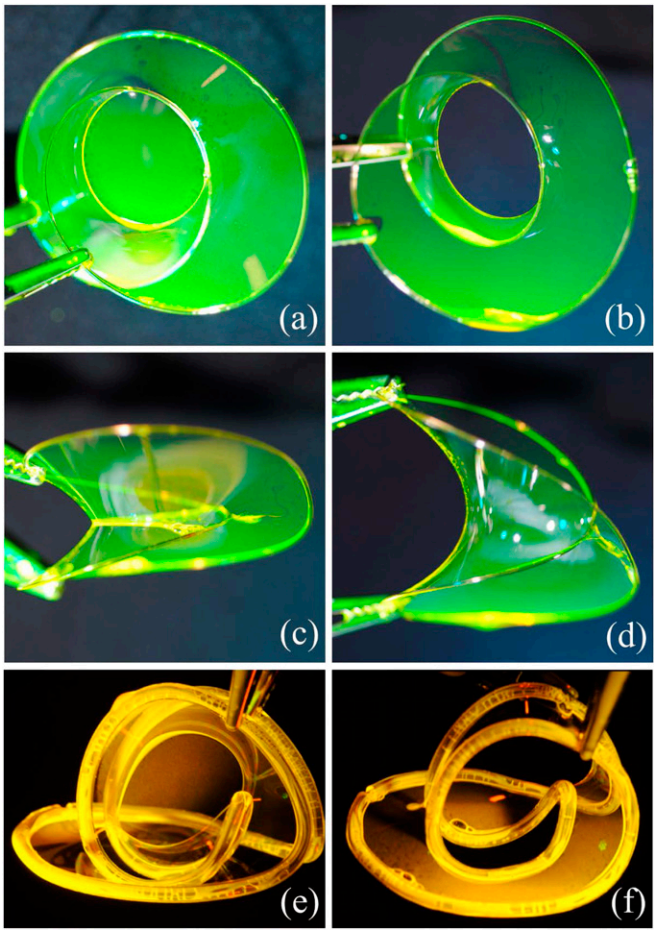

Fig. 2. Soap films. Top (*A* and *B*) and side (*C* and *D*) views of Möbius surfaces with and without secondary film. (*E* and *F*) Punctured Klein-bottled surfaces with and without secondary film.

cases we find that the singularity or singularities are indeed located at the frame. These dynamical evolutions are shown in Movies S1 and S2 (Möbius) and S3 and S4 (punctured Klein).

To quantify the collapse of a neck to the boundary, we determined from each triangulated surface the narrowest diameter D of the neck measured from the point of the eventual location of the singularity to the point on the shortest noncontractible geodesic of the neck at which the normal is the generating vector of the line that joins both points (Fig. 4). That geodesic, in turn, was found by means of an adaptation of Kirsanov's Matlab program (31) to find the exact geodesics between two specified endpoints on a triangular mesh. To find closed geodesics we implemented an iterative procedure to adjust the positions of three endpoints spaced around the neck until the three geodesic segments formed a single smooth curve. Fig. 4 shows the projections of the geodesics onto the x–y plane and the neck diameter D for the Möbius collapse as a function of iteration number of the relaxation scheme. Observe that the stationary right-hand section of the curves in Fig. 4*B* are the sections that the geodesics share with the boundary. The results indicate a clear collapse to the boundary in finite time. While the data appear consistent with a power-law variation of D with time, with a sublinear exponent, at present there is insufficient resolution to determine that exponent more precisely.

As we have mentioned before, motion by mean curvature cannot faithfully represent a bulk singularity in a physical film because in such a film the effects of air pressure have a crucial role in the last stages of the collapse when a Rayleigh instability is triggered and the film produces a satellite drop (or cascade of drops with a cut-off controlled by the parameters of the film) (1, 22). The difference between this singularity and the boundary one that makes the latter amenable to description with mean curvature flow is that physical effects other than surface tension, for instance thickness variations in the film, become relevant only after the singularity has fully developed. In fact, the reconnection of the Plateau border in the collision with the boundary occurs after the surface has reached the location of the singularity.

Location of singularity. Systoles, or the shortest noncontractible geodesics, have been extensively studied in the context of general closed orientable Riemannian manifolds (24). In fact, inequalities relating the systole's length to the surface area and volume of the manifold are well known. Each one of the shortest noncontractible closed geodesics that we used to characterize the neck evolution under mean curvature flow is an example of an LSRB, as defined in the Introduction. While up until now we have only found each local systole as the neck shrinks, it is also possible to find the one such curve on the stable minimal surface before the onset of the instability.

Fig. 5 shows the local systoles for stable minimal punctured Klein (Fig. 5 *A* and *B*) and Möbius band (Fig. 5*C*) surfaces, where for the latter the systole is unique. In the case of the punctured Klein bottle we show only one systole—the second is a mirror image across the central vertical plane of symmetry. When the frame parameters are slightly beyond their critical values and the surfaces start their dynamic evolution toward the collapse, the systoles of the stable configurations can be viewed as the initial conditions for the successive family of systoles described in the previous subsection. A notable feature of each and every one of these systoles, including the one corresponding to the stable minimal surface, is that they are topologically linked to the boundary. In the case of the Möbius strip embedded in space, it can be shown that all noncontractible curves are in fact linked to the boundary. It is this linkage that provides a predictor of the location of the singularity. In fact, in the classic instability of the catenoid produced by pulling the two rings apart, in which the systoles are never linked to the boundary, the singularities occur in the bulk. Moreover, when catenoid collapse is forced by tilting the rings to induce a quasistatic boundary singularity, the systole eventually attaches itself to the boundary immediately before the surface reaches the singularity point; since this evolution has a stable minimal surface at all times, the position of

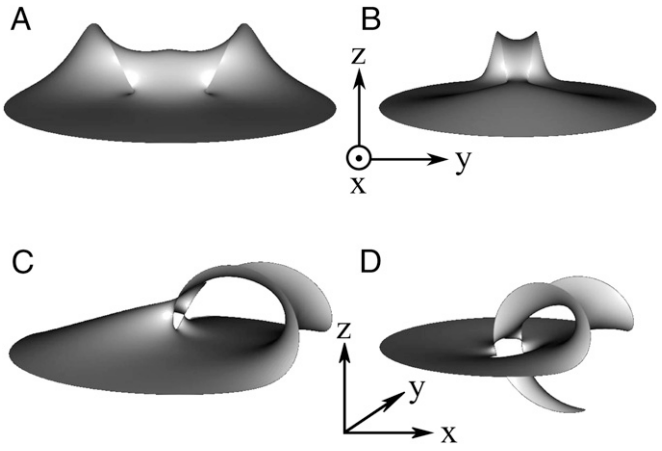

Fig. 3. Numerically obtained minimal punctured Klein surfaces. (*Upper*) Varying the parameter λ for $t = 3.5$. (*A*) $\lambda = 10$ and (*B*) $\lambda = 120$. (*Lower*) Varying t for $\lambda = 10$. (*C*) $t = 3$ and (*D*) $t = 5$.

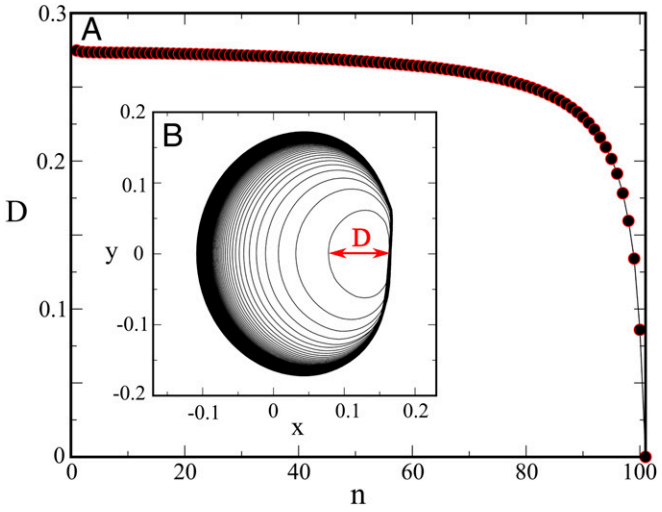

Fig. 4. Collapse dynamics of a Möbius surface from Surface Evolver (30). (*A*) Diameter of the projection of geodesics (*B*) onto the *x*–*y* plane (Fig. 3) as a function of iteration number *n* in the relaxation scheme. The singularity appears at the boundary at a finite time.

the systole before collapse also gives, even though trivially, an accurate prediction of the type of singularity.

The reason systoles are important and useful in the prediction of the character of the motion may be understood through the following heuristic argument: The curvature associated with the systole is exactly canceled by its conjugate curvature when the surface is minimal. When the surface becomes unstable, this delicate balance is broken and it will move with a speed that varies from point to point, driven by the Laplace pressure difference, which is itself proportional to the mean curvature (note that both in mean curvature flow and in more realistic models it is this pressure difference that determines the surface velocity). Since in the unstable regime the points with the largest mean curvature are generically those on the systole, they will move fastest and reach the singularity first by shrinking to a point. Furthermore, because of this shrinkage of the systole and the impossibility of any point on the surface traversing the boundary, the topological linkage of the systole and the boundary automatically determines the character (bulk or boundary) of the singularity.

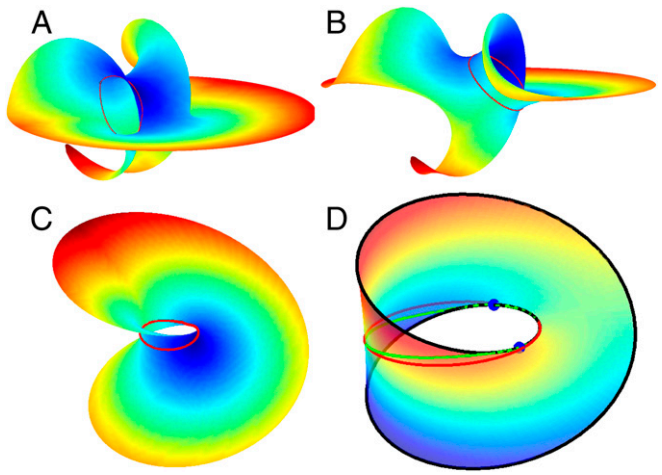

Fig. 5. Systoles on minimal surfaces. (*A* and *B*) Two views of a punctured Klein bottle surface with a systole (red line). (*C*) Systole for a Möbius minimal surface. (*D*) Systole (green) and approximate systole (red) for a ruled surface in the shape of a Möbius band. Blue dots indicate loci where the geodesic curvature changes sign. The color scheme represents the *z* coordinate of points on surfaces.

Given that the Möbius band is the paradigm for singularity formation at the boundary, it follows that having an analytic result for the systoles of this surface, even an approximate one, is very desirable. With this mind we have used the ruled surfaces (32) generated by Eq. **1**, where now $-1 \le \mu \le 1$ (11). With the surface specified by the vector $\mathbf{x}(\mu,\theta)$, the length L of a curve on that surface is

$$L = \int_0^{2\pi} d\theta \left[E\left(\frac{d\mu}{d\theta}\right)^2 + 2F\frac{d\mu}{d\theta} + G \right]^{1/2}, \qquad [3]$$

where $E = \mathbf{x}_\mu \cdot \mathbf{x}_\mu$, $F = \mathbf{x}_\mu \cdot \mathbf{x}_\theta$, and $G = \mathbf{x}_\theta \cdot \mathbf{x}_\theta$ are the coefficients of the first fundamental form. To find the geodesic, we use a relaxation dynamics with L as a Lyapunov function,

$$\mu_t = -\frac{\delta L}{\delta \mu}. \qquad [4]$$

Fig. 5*D* shows the numerically obtained geodesic for the case $\tau = 0.4$. Observe that the solution hugs the boundary over a finite arc. This is consistent with the general result that a geodesic cannot touch the boundary if the geodesic curvature κ_g of the boundary is positive, supported by the following argument. Suppose $\mathbf{\Gamma}(s)$ is a geodesic curve in a surface Σ, parametrized by arc length s. Then the second derivative of $\mathbf{\Gamma}$ is normal to Σ, for otherwise, we could shrink $\mathbf{\Gamma}$ by pushing it in the direction of the second derivative. If $\mathbf{\Gamma}$ touches the boundary at a convex point, then the second derivative of $\mathbf{\Gamma}$ in the direction normal to the boundary but tangent to Σ must be positive, and we can shrink $\mathbf{\Gamma}$ by gently pushing it in that direction. It follows that moving a geodesic in the direction of the second derivative when the boundary curvature is negative will push the curve off the surface. Hence, negative geodesic curvature of the boundary is a necessary but not sufficient condition for the systole to touch it. In the present case, a straightforward calculation shows that

$$\kappa_g = A(\tau) + B(\tau)\cos\theta + C(\tau)\cos 2\theta, \qquad [5]$$

where A, B, and C are polynomials in τ. One can verify that the region of θ over which the numerical geodesic coincides with the boundary does indeed lie within the region of negative κ_g.

A remarkably good analytic approximation to the systole on the ruled surface can be obtained by first finding a curve whose tangent vector is everywhere orthogonal to both the surface normal and the lines of constant μ. Such a curve does not lie on the surface. However, as the binormal to that curve is constant, it lies in a plane, which can be easily found. The approximate geodesic is then found as the intersection of the ruled surface and that plane. This curve can be expressed explicitly in terms of its Cartesian components or parametrically in the form $\mu(\theta;\tau)$ by first defining

$$g(\tau) = \frac{2(1-\tau)}{\tau + 2(1-\tau)^2}, \qquad [6a]$$

$$\cos\theta^* = 1/g. \qquad [6b]$$

If Eq. **6b** has real solutions for θ^* (which occurs for $0 \le \tau \le 1/2$), then the geodesic is defined piecewise:

$$\mu(\theta) = \begin{cases} -g(\tau)\cos\theta & |\theta| \ge \theta^* \\ -1 & \text{otherwise} \end{cases}. \qquad [7]$$

Note that this ruled surface has the nonphysical feature of self-intersection for $\tau > \tau_s \simeq 0.58$. For $1/2 < \tau < \tau_s$, the approximate geodesic does not touch the boundary, and has the

form $\mu(\theta) = -g\cos\theta$. This is shown overlaid in red in Fig. 5. As with the numerically obtained geodesic, the region of coincidence with the boundary lies within the domain of negative geodesic boundary curvature, as required.

Conclusions

By identifying examples of boundary singularities, other than the collapse of the Möbius band, that occur when there is a topological change in soap films spanning a wire, we have made a first attempt at classifying them. Besides the well-known bulk singularity we found two other types—quasistatic and catastrophic—both occurring at the boundary. We found strong evidence that any catastrophic singularity which develops a neck will asymptotically converge to a Möbius-like singularity. Furthermore, numerical studies showed that motion by mean curvature exhibits boundary singularities, reproducing the experimental findings. We also found that the predictor of the position of the singularity was the linkage between the boundary and the systole of the last stable surface before the onset of instability.

Clearly, these results are not in a rigorous framework, but provide insight into which variables have a role in the transition. They also suggest that among the singularity types, the one corresponding to the quasistatic boundary should be the less difficult to study because it is the one for which it is possible to construct a family of stable minimal surfaces at all times. An important goal is to rigorously establish the conditions under which mean curvature motion leads to a boundary singularity. A more modest goal is to prove, in the context of the Mobius surface we have parametrized, that motion by mean curvature produces a singularity at the boundary.

ACKNOWLEDGMENTS. We thank M. Gromov for comments on systoles on bounded surfaces, L. Guth for suggesting the connection between boundary curvature and systoles, R. Kusner and F. Morgan for discussions on the topology of geodesics, and P. Constantin for discussions on mean curvature flows; D. Page-Croft, C. Hitch, and J. Milton for technical assistance; and K. Brakke, M. Evans, S. Furlan, and A. Kranik for computational assistance. This work was supported by Engineering and Physical Sciences Research Council Grant EP/I036060/1 and the Schlumberger Chair Fund.

1. Eggers J (1997) Nonlinear dynamics and the breakup of free-surface flows. *Rev Mod Phys* 69(3):865–929.
2. Caflisch R, Papanicolaou G, eds (1993) Singularities in fluids, plasmas and optics. *NATO Science Series C*, Proceedings of the NATO Advanced Research Workshop (Springer, New York), Vol. 404.
3. Bajer K, Moffatt HK, eds (2002) Tubes, sheets and singularities in fluid dynamics. *Fluid Mechanics and Its Applications*, Proceedings of the NATO Advanced Research Workshop (Kluwer, London), Vol. 71.
4. Mermin ND (1979) The topological theory of defects in ordered media. *Rev Mod Phys* 51(3):591–648.
5. Arnold VI (1991) *The Theory of Singularities and Its Applications* (Cambridge Univ Press, Cambridge, UK).
6. Langer SA, Sethna JP (1986) Textures in a chiral smectic liquid-crystal film. *Phys Rev A* 34(6):5035–5046.
7. Kasamatsu K, Takeuchi H, Tsubota M, Nitta M (2013) Wall-vortex composite solitons in two-component Bose-Einstein condensates. *Phys Rev A* 88(1):013620.
8. Pettey D, Lubensky TC (1999) Stability of texture and shape of circular domains of Langmuir monolayers. *Phys Rev E Stat Phys Plasmas Fluids Relat Interdiscip Topics* 59(2):1834–1845.
9. Sakai N, Tong D (2005) Monopoles, vortices, domain walls and D-branes: The rules of interaction. *JHEP* 03:019.
10. Goldstein RE, Moffatt HK, Pesci AI (2012) Topological constraints and their breakdown in dynamical evolution. *Nonlinearity* 25(10):R85–R98.
11. Goldstein RE, Moffatt HK, Pesci AI, Ricca RL (2010) Soap-film Möbius strip changes topology with a twist singularity. *Proc Natl Acad Sci USA* 107(51):21979–21984.
12. Courant R (1938) The existence of a minimal surface of least area bounded by prescribed Jordan arcs and prescribed surfaces. *Proc Natl Acad Sci USA* 24(2):97–101.
13. Courant R (1940) Soap film experiments with minimal surfaces. *Am Math Mon* 47(3):167–174.
14. Colding TH, Minicozzi WP (2012) Generic mean curvature flow I; Generic singularities. *Ann Math* 175(2):755–833.
15. Leppinen D, Lister JR (2003) Capillary pinch-off of inviscid fluids. *Phys Fluids* 15(2):568–578.
16. Nitsche M, Steen PH (2004) Numerical simulations of inviscid capillary pinchoff. *J Comput Phys* 200(1):299–324.
17. Gage M (1984) Curve shortening makes convex curves circular. *Invent Math* 76(2): 357–364.
18. Gage M, Hamilton RS (1986) The heat equation shrinking convex plane curves. *J Diff Geom* 23(1):69–96.
19. Grayson MA (1987) The heat equation shrinks embedded plane curves to round points. *J Diff Geom* 26(2):285–314.
20. Huisken G (1984) Flow by mean curvature of convex surfaces into spheres. *J Diff Geom* 20(1):237–266.
21. Cryer SA, Steen PH (1992) Collapse of the soap-film bridge: Quasistatic description. *J. Colloid Int. Sci.* 154(1):276–288.
22. Chen YJ, Steen PH (1997) Dynamics of inviscid capillary breakup: Collapse and pinchoff of a film bridge. *J Fluid Mech* 341:245–267.
23. Robinson ND, Steen PH (2001) Observations of singularity formation during the capillary collapse and bubble pinch-off of a soap film bridge. *J Coll Int Sci* 241(2): 448–458.
24. Gromov M (1983) Filling Riemannian manifolds. *J Diff Geom* 18(1):1–147.
25. Guth L (2010) Metaphors in systolic geometry. arXiv:1003.4247.
26. Berger M (2008) What is, . . ., a systole? *Not Am Math Soc* 55(3):374–376.
27. Almgren FJ (2001) *Plateau's Problem: An Invitation to Varifold Geometry* (American Mathematical Society, Providence, RI), revised edition.
28. Weaire D, Rivier N (1984) Soap, cells and statistics - random patterns in two dimensions. *Contemp Phys* 25(1):59–99.
29. Maggioni F, Ricca RL (2006) Writhing and coiling of closed filaments. *Proc R Soc A* 462(2074):3151–3166.
30. Brakke K (1992) The Surface Evolver. *Exp Math* 1(2):141–165.
31. Kirsanov D (2007) Exact geodesic for triangular meshes, Matlab file exchange. Available at www.mathworks.co.uk/matlabcentral/fileexchange/18168-exact-geodesic-for-triangular-meshes. Accessed May 2, 2014.
32. Edge WL (1931) *The Theory of Ruled Surfaces* (Cambridge Univ Press, Cambridge, UK).